ISSN 1590-2595
anno 2020 numero 162

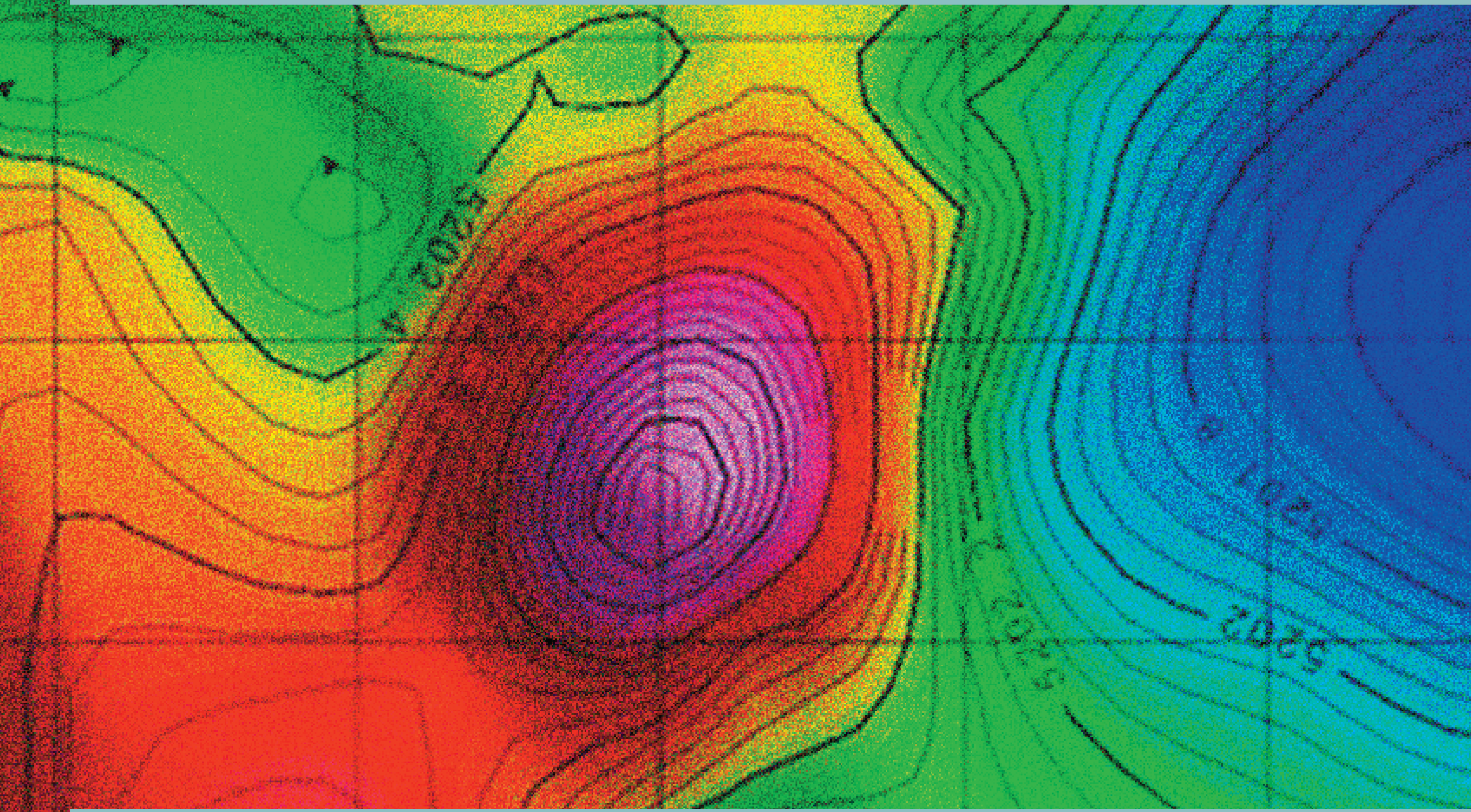

# QUADERNI di GEOFISICA

## Application of PSO Algorithm based on the mean value of maximum frequency distribution for 2-D inverse modeling of gravity data due to a finite vertical cylinder shape

162

ISTITUTO NAZIONALE DI GEOFISICA E VULCANOLOGIA

**Direttore Responsabile**
Valeria DE PAOLA

**Editorial Board**
Luigi CUCCI - Editor in Chief (luigi.cucci@ingv.it)
Raffaele AZZARO (raffaele.azzaro@ingv.it)
Christian BIGNAMI (christian.bignami@ingv.it)
Mario CASTELLANO (mario.castellano@ingv.it)
Viviana CASTELLI (viviana.castelli@ingv.it)
Rosa Anna CORSARO (rosanna.corsaro@ingv.it)
Domenico DI MAURO (domenico.dimauro@ingv.it)
Mauro DI VITO (mauro.divito@ingv.it)
Marcello LIOTTA (marcello.liotta@ingv.it)
Mario MATTIA (mario.mattia@ingv.it)
Milena MORETTI (milena.moretti@ingv.it)
Nicola PAGLIUCA (nicola.pagliuca@ingv.it)
Umberto SCIACCA (umberto.sciacca@ingv.it)
Alessandro SETTIMI (alessandro.settimi1@istruzione.it)
Andrea TERTULLIANI (andrea.tertulliani@ingv.it)

**Redazione**
Francesca DI STEFANO - Coordinatore
Rossella CELI
Barbara ANGIONI
Patrizia PANTANI
Massimiliano CASCONE

redazionecen@ingv.it

**REGISTRAZIONE AL TRIBUNALE DI ROMA N.174 | 2014, 23 LUGLIO**

© 2014 INGV Istituto Nazionale di Geofisica e Vulcanologia
Rappresentante legale: Carlo DOGLIONI
Sede: Via di Vigna Murata, 605 | Roma

ISTITUTO NAZIONALE DI GEOFISICA E VULCANOLOGIA

ISSN 1590-2595
anno **2020** numero **162**

QUADERNI di GEOFISICA

# Application of PSO Algorithm based on the mean value of maximum frequency distribution for 2-D inverse modeling of gravity data due to a finite vertical cylinder shape

Ata Eshaghzadeh[1], Sanaz Seyedi Sahebari[2]

[1]Geophysicist at Zima Company, Chaloos, Iran
[2]Roshdiyeh Higher Education Institute, Tabriz, Iran

Accepted 9 January 2020 | *Accettato 9 gennaio 2020*

How to cite | *Come citare* Eshaghzadeh A., Seyedi Sahebari S., (2020). Application of PSO Algorithm based on the mean value of maximum frequency distribution for 2-D inverse modeling of gravity data due to a finite vertical cylinder shape. Quad. Geofis., 162: 1-22, https://doi.org/10.13127/qdg/162

Cover The Bouguer gravity anomalies map | *In copertina Mappa dell'anomalia gravitazionale di Bouguer*

162

# INDEX

| | |
|---|---|
| **Abstract** | **7** |
| **Introduction** | **7** |
| **1. Forward modeling** | **8** |
| **2. Particle Swarm Optimization (PSO)** | **8** |
| **3. Theoretical example** | **10** |
| **4. Gravity anomaly due to chromite deposit** | **12** |
| **5. Gravity anomaly due to Louisiana salt dome** | **15** |
| **6. Discussion and Conclusions** | **17** |
| **References** | **18** |

# Abstract

In this paper, Particle Swarm Optimization (PSO) algorithm is employed to invert the gravity anomaly due to a finite vertical cylinder source. The PSO inversion determines the radius (R), density contrast (ρ), depth to top (z) and bottom (h) parameters of a gravity anomaly causative body and also the location of anomaly source (origin $_{x0}$) and gravity value in the origin ($g_{x0}$) whose amount is maximum. During an iterative process, PSO estimates the subsurface model parameters and the gravity response according to them at each iteration. A profound weak point of Particle Swarm Optimization method is getting into local minimum as the PSO algorithm can not estimates the optimal solutions. In order to overcoming this problem, the code is run frequently and the abundance distributions of the estimated values for the different parameters is drawn. Average value of each range whose frequently distributions is maximum are considered as best solution. To evaluate the proficiency of the PSO method, a finite vertical cylinder synthetic model has been considered as the satisfactory results were achieved for the noise-free and noise-corrupted gravity data. We have also applied this approach for inverse modeling two real gravity anomaly due to a chromite deposit mass, situated east of Sabzevar, Iran and a salt dome offshore titled Louisiana from USA.

Keywords Chromite, Finite vertical cylinder, Gravity, Particle Swarm Optimization (PSO), Salt dome

## Introduction

Particle Swarm Optimization (PSO) is a relatively recent method and one of the most popular nature-inspired heuristic optimization algorithm developed by James Kennedy and Russell Eberhart in 1995. PSO has few applications to geophysical problems [Alvarez et al., 2006; Shaw and Srivastava, 2007]. However, PSO has been successfully employed in some fields of geophysics, such as inversion of self-potential of idealized bodies'anomalies [Monteiro Santos, 2010], gravity inversion of a fault by Particle Swarm Optimization [Toushmalani, 2013a and b], gravity inversion and uncertainty assessment of basement relief via Particle Swarm Optimization [Pallero et. al., 2015], application of particle swarm optimization for gravity inversion of 2.5-D sedimentary basins [Singh and Singh, 2017], 2D dipping dike magnetic data interpretation using a robust particle swarm optimization [Essa and El-Hussein, 2017], inversion of residual gravity anomalies using tuned PSO [Roshan and Singh, 2017], gravity data interpretation using PSO [Essa and El-hussein, 2018], and PSO (Particle Swarm Optimization) for interpretation of magnetic anomalies caused by simple geometrical structures [Essa and El-Hussein, 2018].

We have applied the Particle Swarm Optimization algorithm to interpret the gravity anomaly caused by a buried mass with a geometric shape of the finite vertical cylinder. The radius (R), density contrast (ρ), depth to top (z) and bottom (h), axis location ($x_0$) and gravity value in the origin ($g_{x0}$) are the model parameters which are computed. In order to achieve the optimal solutions, we have proposed a statistical strategy based on the mean value of maximum frequency distribution. In this scheme, a gravity data set interprets using PSO algorithm for several times and the estimated model parameters classify in the predefined ranges. The mean value of the estimates of each parameter which lie in a range with the most frequency distribution is selected as the best solution. Thus, using this approach can overcome the weaknesses of PSO, that is,

fall into local minimum easily. In fact, the ranges with the less frequency distribution include mostly the incorrect responses.
The proposed method is tested for the theoretical gravity data related to a finite vertical cylinder model, with and without added random noise, and also two real gravity data from Iran and USA. For this purpose, a MATLAB code has been developed.

# 1. Forward modeling

The gravity effect of a finite vertical cylinder is defined by Hammer (1974)

$$g(\mathrm{x}) = KF(\mathrm{x}) \qquad (1)$$

Where k is amplitude coefficient as

$$F(x_i) = \frac{1}{\sqrt{x^2+z^2}} - \frac{1}{\sqrt{x^2+h^2}}, \quad \mathrm{K} = \ \mathrm{G}\pi\mathrm{R}^2$$

where x is the horizontal location coordinate of measurement points, z and h represent the depths to the top and base planes of causative structure from ground surface respectively, G is the gravitational constant, R is the radius of the horizontal cross section of a vertical cylinder, and ρ is the density contrast (Figure 1).

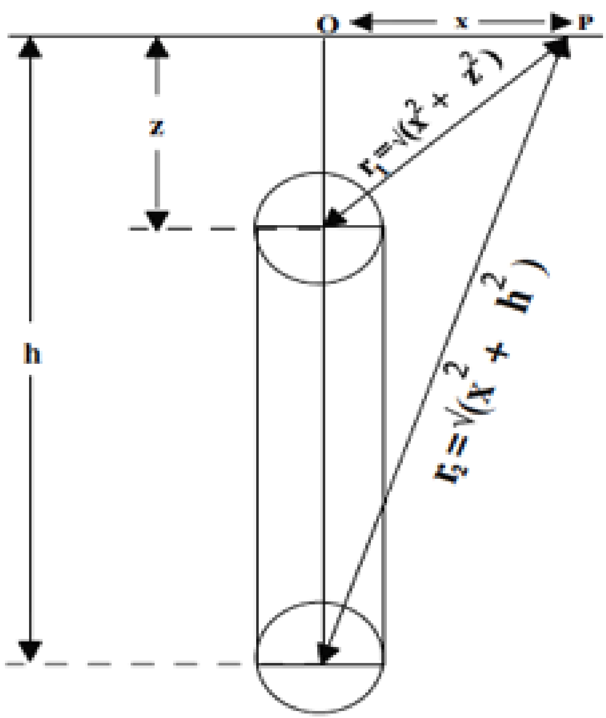


**Figure 1** Geometries of the finite vertical cylinder.

# 2. Particle Swarm Optimization (PSO)

Particle Swarm Optimization (PSO) is a crowd based on stochastic optimization procedure, which is inspired by the social behavior of the particles such as a swarm of bird, flocking bees, and fish schooling.

The location of each particle (parameter) as one of the potential computational variables in the PSO algorithm, changes at each iteration of the evaluation process. In the other words, this position is refreshed during the iteration trend so that the particle reaches its best position which is known as Pbest (particle best value) and the best region in the group which is known as Gbest (best value in the group or global best value) among the Pbest. Accordingly, each particle endeavors to adjust its situation in the present velocity of the operation of the algorithm.
To obtain a new position of the particle, the velocity of the particle is updated using the following equations, given by Sweilam et al. [2007]

$$V_i^{t+1} = wV_i^t + c_1 rand()(\mathrm{P}best_i - X_i^t) + c_2 rand()(\mathrm{G}best_i - X_i^t) \quad (2)$$

$$X_i^{t+1} = X_i^t + V_i^{t+1} \quad (3)$$

Where, $V_i^t$ is the present velocity of the individual (particle) *i* at the $t_{th}$ iteration, $X_i^t$ is the current position of the $i_{th}$ particle at the $t_{th}$ iteration, rand() is a random number between 0 and 1, $c_1$ and $c_2$(learning factors) are positive constant numbers known as cognitive coefficient and social coefficient, respectively, which control the individual and the social behavior and *w* is an inertial coefficient whose value is usually slightly less than 1 [Monteiro Santos, 2010]. Generally, the Pbest and Gbest are accelerated by two operators $c_1$ and $c_2$, and two random numbers produced between [0, 1] whereas the current movement is multiplied by an inertia factor *w*. For *w*, the minimum ($w_{min}$) and maximum ($w_{max}$) limits are defined, in the PSO algorithm until its amount is bounded in the range ($w_{min}$,$w_{max}$) at each repetition.
Alteration of the inertia weight of the particle is performed by a decreasing strategy linearly at each iteration in the following form [Shi and Eberhart, 1998]

$$w = w_{\max} - (w_{\max} - w_{\min}) \times \frac{t_{it}}{T_{\max}} \quad (4)$$

where $t_{it}$ is current iteration, and $T_{max}$ is the maximum number of iteration.
Such said, the fundamental procedure of PSO algorithm lies in quickening each individual towards its Pbest and the Gbest positions with a random weighted acceleration at each iteration. It is worth of note that the maximum velocity ($V_{max}$) indicates the highest amount of location coordinates variation that can take place during each iteration. As a matter of fact, the concept of maximum velocity was introduced to avoid outflow and divergence [Das et al., 2008].
When the differences between the observed gravity field data and the generated one from the estimated model is minimized, the best exact values of the particles (model parameters) are obtained. For this purpose, we use the following simple objective function:

$$Q = \frac{2\sum_i^N \left| g_i^o - g_i^c \right|}{\sum_i^N \left| g_i^o - g_i^c \right| + \sum_i^N \left| g_i^o + g_i^c \right|} \quad (5)$$

Where N is the number of the gravity measurement point, $g_i^o$ and $g_i^c$ are the gravity anomaly observed and calculated at the point $P(x'_i)$, respectively.

The learning factors ($c_1$ and $c_2$) are traditionally both equal to 2 [Sweilam et al., 2007]. However, based on recent literature, electing $c_1$ more predominant than $c_2$ and $c_1 + c_2 \leq 4$ may present better conclusions [Parsopoulos and Vrahatis, 2002].

## 3. Theoretical example

Figure 2a shows the calculated theoretical gravity field variations with 1 m interval along a 100 m profile due to an initial finite vertical cylinder model with the parameters z=30 m, h=60 m and R=10 m (Figure 2b), where the maximum gravity is the center of the profile. The density contrast is given as ρ=1000 kg/m$^3$.
According to the defined search ranges for the parameters, as shown in Table 1, one hundred and twenty primary models were randomly manufactured. These ranges include the values assumed for the initial model. The code is performed two hundred times. Figure 3 shows the frequency charts of the various parameters estimates for some range of solutions. With attention to Figure 3, the most abundant distributions of the radius (R), depth to top (z) and bottom (h) parameters, location of mass ($x_0$), gravity value in the origin ($g_{x0}$) and density contrast (ρ) have been occurred in the ranges of 9.5 to 10.5 m, 28 to 33 m, 58 to 63 m, -0.5 to 0.5 m, 0.034 to 0.036 mGal and 975 to 1025 kg/m$^3$, respectively. Based on the strategy of the mean value of the maximum frequency distribution, considering the forgoing ranges, the obtained parameters values from the Particle Swarm Optimization algorithm solutions are given as z=29.96 m, h=60.12 m, R=10.01 m, $x_0$=0.014 m, $g_{x0}$=0.03541 mGal and ρ=1007 kg/m$^3$. Figure 2a shows the generated gravity anomaly from the inferred structure using PSO inversion which is displayed in Figure 2b as is similar initial model.
The numerical output of the PSO inversion has been brought in Table 1. The error estimated by the objective function for the noise-free synthetic gravity data is 0.0036.

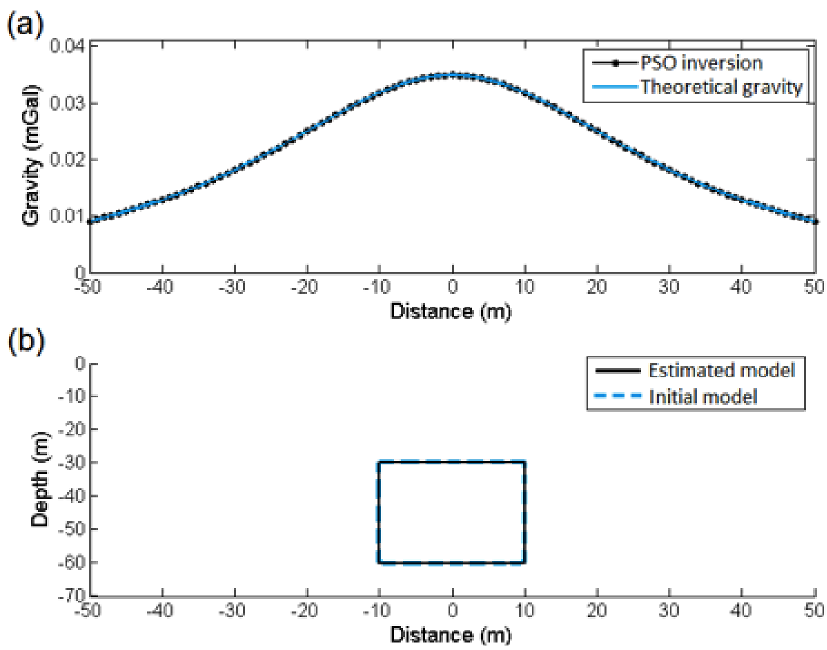


**Figure 2** (a) Theoretical gravity and inverted gravity using PSO due to (b) initial and estimated finite vertical cylinder models.

The effect of error on the performance of the PSO is investigated by adding 10% noise to the gravity response of the finite vertical cylinder model by following equation:

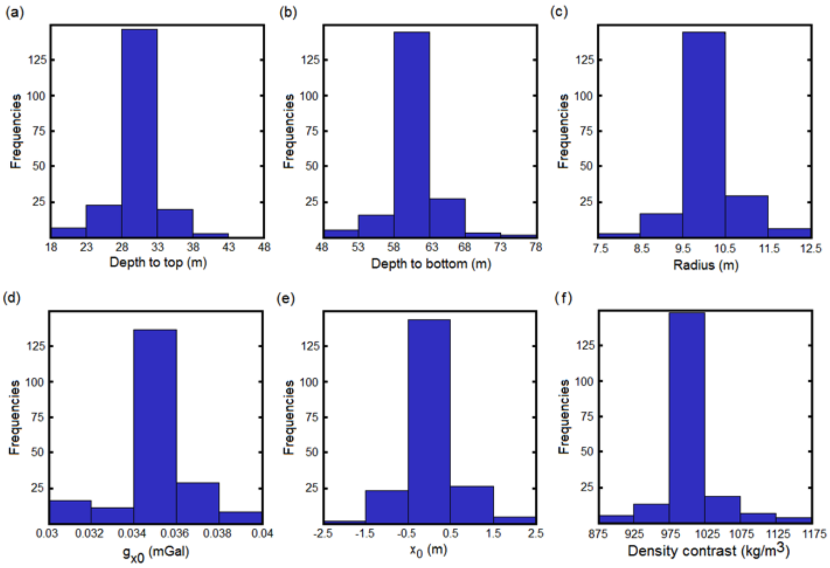


**Figure 3** Frequency distribution of the various parameters solutions a) depth to top (m) b) depth to bottom (m) c) radius (m) d) gravity value in the origin (mGal) e) location of mass (m) f) density contrast (kg/m$^3$) for the theoretical gravity data.

$$g_{noise}(x_i) = g(x_i) + M(\mathrm{RAN(i)} - 0.5) \quad (6)$$

Where, $g_{noise}(X_i)$ is the noisy gravity anomaly value at $x_i$, M control the noise level (here M is 10) and RND(i) is a pseudo-random number whose range is (0, 1).

The maxima frequency distributions ranges achieved for 10% noise corruption gravity data is similar to noise-free gravity data, except the radius parameter whose most solutions lie in the range 9 to 11 m (Figure 4). According to Figure 4, the resulted parameters values from the Particle Swarm Optimization algorithm solutions, based on strategy of mean value of maximum frequency distribution, are z=30.9 m, h=60.4 m, R=10.3 m, $x_0$=-0.021 m, $g_{x0}$=0.0351 mGal and ρ=985 kg/m$^3$. The contaminated gravity data and inverted noisy responses by the PSO are shown in Figure 5a. The simulated structure using PSO inversion for noise-corrupted gravity data is shown in Figure 5b. The numerical results are presented in Table 1. The error estimated by the objective function for the noisy gravity data is 0.061.

The satisfactory estimated parameters from the noise-free and 10% noise corruption synthetic gravity data demonstrate the acceptable proficiency of the PSO inversion method based on the mean value of the maximum frequency distribution.

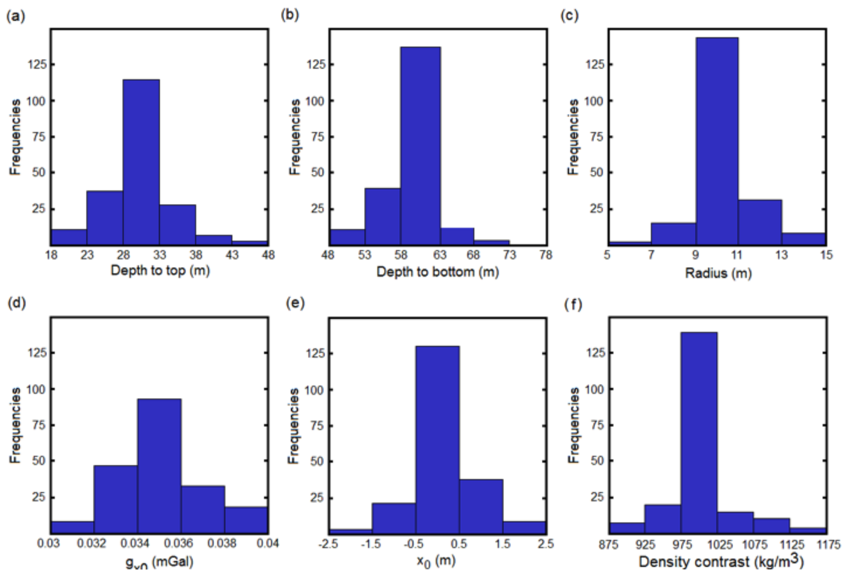


**Figure 4** Frequency distribution of the various parameters solutions a) depth to top (m) b) depth to bottom (m) c) radius (m) d) gravity value in the origin (mGal) e) location of mass (m) f) density contrast (kg/m$^3$) for noise corrupted theoretical gravity data.

## 4. Gravity anomaly due to chromite deposit

The site under survey is located in the east of Iran, around Sabzevar. The outcomes of the stones in this area are mostly the alkali and ultrabasic igneous rocks and ophiolite as the chromite mineralization can be found in these rocks (Figure 6). In this region, the chromite deposits are massive. Figure 7 shows the Bouguer gravity anomalies map of the area under consideration where an average density of 2.7 gr/cm$^3$ was considered for Bougure slab correction [Eshaghzadeh et al., 2019]. The gravity measurement was done along 12 profiles with a station interval of about 10 m. The gravity data cover a 120×100 m area of the exploration region in Sabzevar.

**Figure 5** (a) 10% noise-corrupted theoretical gravity and inverted gravity using PSO due to (b) initial and estimated finite vertical cylinder models.

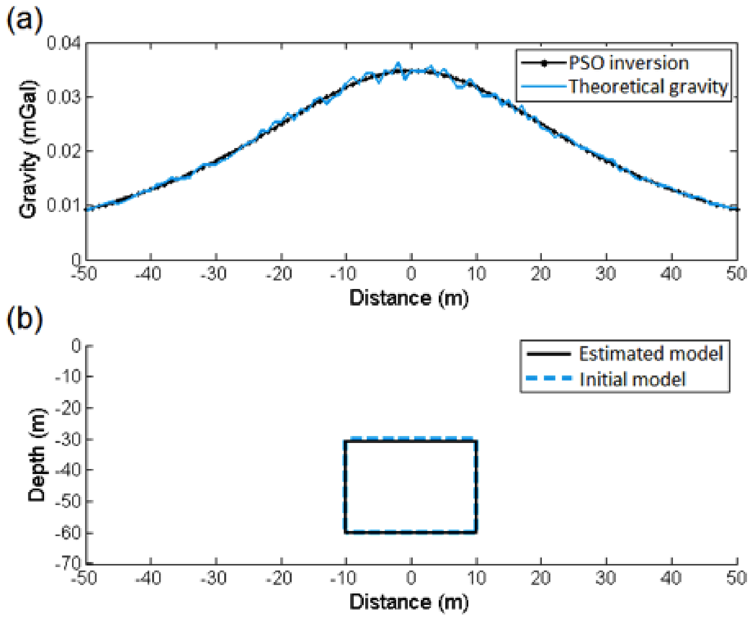


| Parameter | Q | Z (m) | h (m) | R (m) | ρ (kg/m$^3$) | $g_{x0}$ (mGal) | $x_0$ (m) |
|---|---|---|---|---|---|---|---|
| Ranges | - | 18 - 48 | 48 - 78 | 5 - 15 | 800 -1200 | 0.03 – 0.04 | -2.5 to 2.5 |
| Noise free | 0.0036 | 29.96 | 60.12 | 10.01 | 1007 | 0.03543 | 0.014 |
| 10% noise | 0.061 | 30.9 | 60.4 | 10.3 | 985 | 0.0351 | -0.021 |

**Table 1** The assumed search ranges and numerical results interpreted by PSO for the theoretical gravity data, with and without random noise.

For reaching to the residual gravity anomalies which is our desire, the regional gravity anomalies must be removed using a trend (degree two polynomial) from the Bouguer anomaly. Figure 8 displays the map of the computed local gravity field. The host rock of the chromite has the positive density contrast than the surrounding formation, therefore on the residual gravity anomalies map is appeared as the positive anomaly.

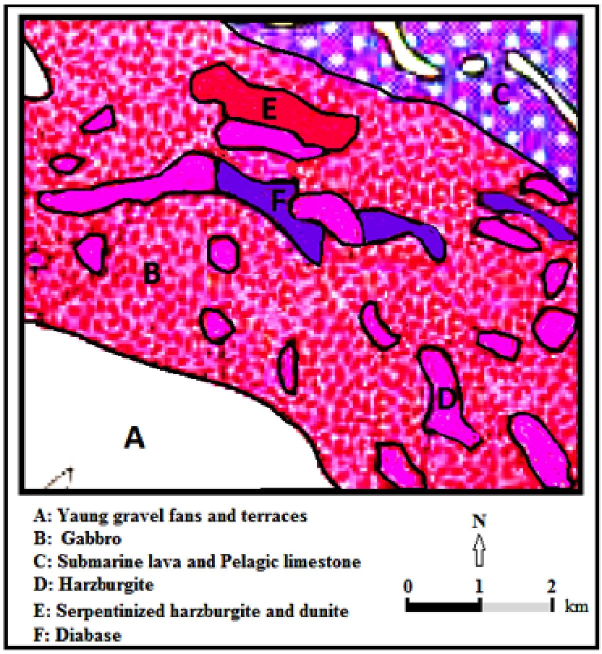


**Figure 6** The geological map of the region under investigation.

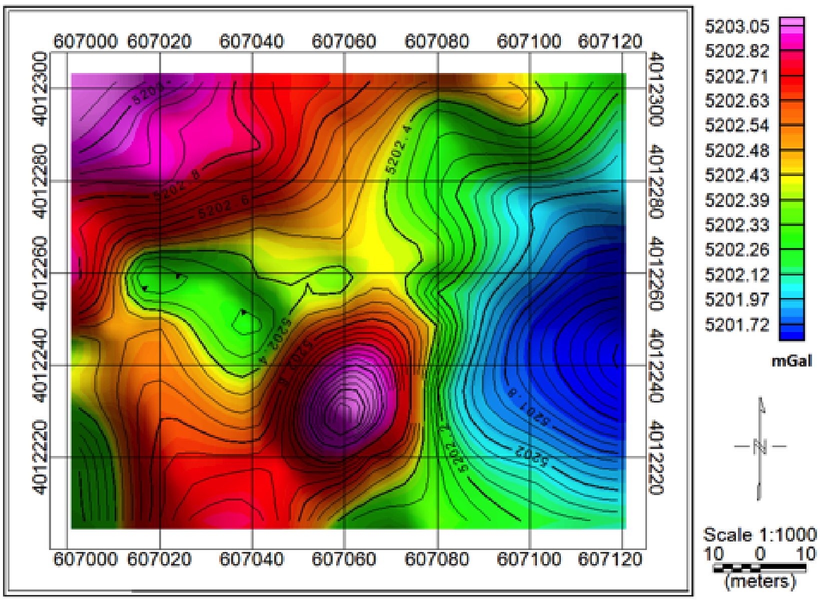


**Figure 7** The Bouguer gravity anomalies map.

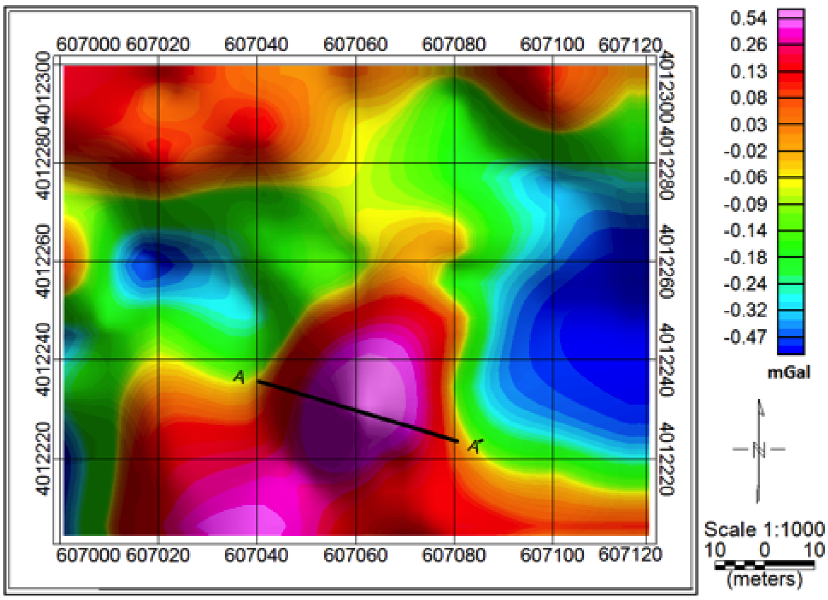


**Figure 8** The residual gravity anomalies map. The profile AA′ is specified with a nearly W-E direction.

The average density of the chromite mass is about 4.6 $gr/cm^3$, whereas the density of the encompassing formation is between 3 $gr/cm^3$ to 3.5 $gr/cm^3$ [Eshaghzadeh et al., 2019]. Here, we analyze the residual gravity anomaly along the profile AA′ using PSO method which runs across the chromite mineral mass in an approximately W–E direction as is shown in Figure 8. The length of profile is 42 m and the gravity sampling interval is given as 2 m.

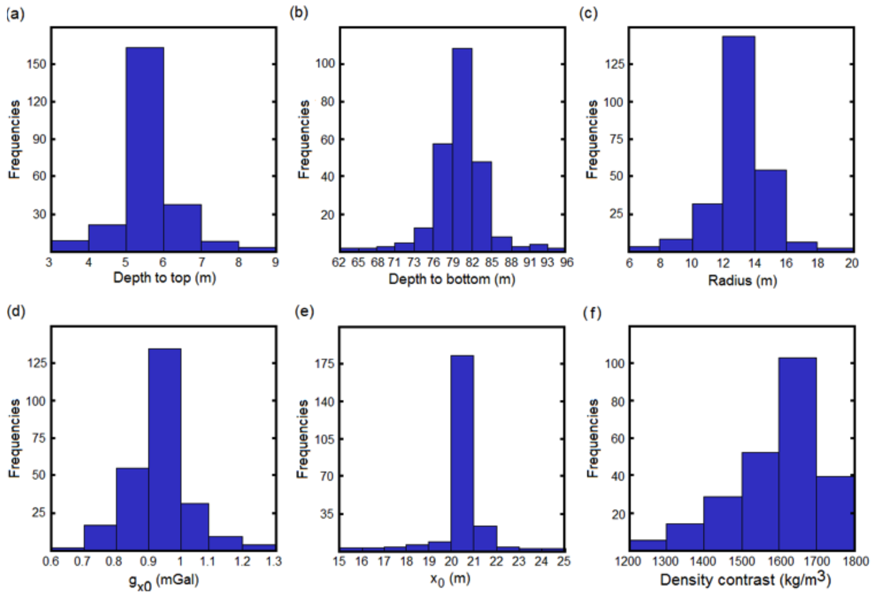


**Figure 9** Frequency distribution of the various parameters solutions a) depth to top (m) b) depth to bottom (m) c) radius (m) d) gravity value in the origin (mGal) e) location of mass (m) f) density contrast ($kg/m^3$) for real gravity data due to the Chromite deposit.

Considering the assumed search ranges for the changeable parameters of the subsurface mass, as have been shown in Table 2, one hundred and fifty primary models were randomly generated. These ranges for the parameters have been chosen based on the geological information. The code has been run two hundred and fifty times. Figure 9 exhibits the frequency distributions of the estimated parameters values in the several range of the solutions. Considering Figure 3, the most solutions value of the radius (R), depth to top (z) and bottom (h) parameters, location of mass ($x_0$), gravity value in the origin ($g_{x0}$) and density contrast (ρ) have been situated in the ranges of 12 to 14 m, 5 to 6 m, 79 to 82 m, 20 to 21 m, 0.9 to 1 mGal and 1600 to 1700 $kg/m^3$, respectively. Based on the strategy of the mean value of the maximum frequency distribution, the evaluated parameters values for the gravity causative mass are z=5.8 m, h=80.4 m, R=13.14 m, $x_0$=20.8 m, $g_{x0}$=0.93 mGal and ρ=1627 $kg/m^3$.
The gravity field variations along profile AA′ as well as the obtained ones from the PSO inversion have been revealed in Figure 10a. The inverted buried structure is shown in Figure 10b.

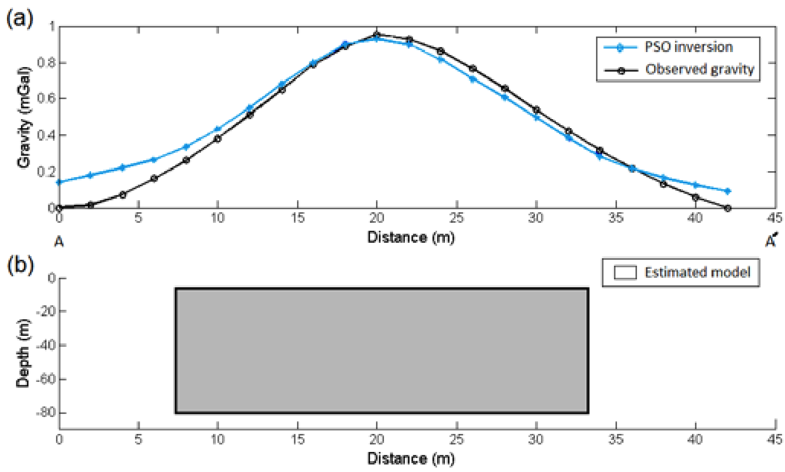


**Figure 10** (a) Observed gravity anomaly along profile AA′, and inverted gravity due to (b) estimated finite vertical cylinder structure using PSO.

The inverted parameters for real gravity using PSO are tabulated in Table 2.

| Parameter | Z (m) | h (m) | R (m) | ρ ($kg/m^3$) | $g_{x0}$ (mGal) | $x_0$ (m) |
|---|---|---|---|---|---|---|
| Ranges | 2 - 10 | 50 - 100 | 5 - 20 | 1200 - 1800 | 0.6 – 1.3 | 15 to 25 |
| Results | 5.8 | 80.4 | 13.14 | 1627 | 0.93 | 20.8 |

**Table 2** The considered search ranges for the anomaly source parameters and the obtained parameters from the PSO inversions.

The Euler deconvolution method is a popular and well known technique in potential field study which is widely used for estimating the depth of the anomaly source. In this study, we have employed the Euler method for calculating the depth of the chromite mass by choosing a structure index of 1 and a window size of 5×5 points. Figure 10 shows the solutions obtained from Euler deconvolution as plotted on the residual gravity anomaly map. The Euler solutions located on the gravity anomaly present a depth between 5 to 10 m for the buried deposit (red points in Figure 11). Thus, the estimated depth to top by the two methods are in a same range.

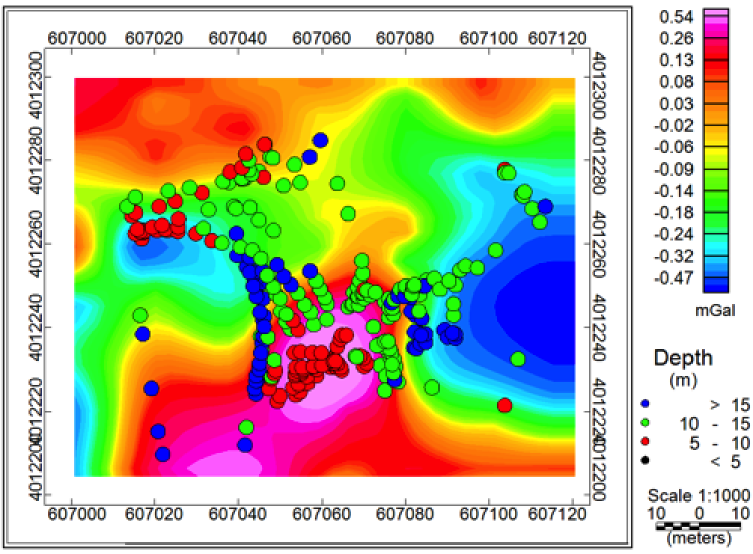


**Figure 11** The depth solutions estimated by the Euler deconvolution method for the residual gravity anomalies.

## 5. Gravity anomaly due to Louisiana salt dome

The second field example is a residual gravity anomaly profile passing over the center of the gravity map offshore Louisiana salt dome situated in USA (Figure 12). We have digitalized the residual gravity field along 13 km profile AA´ at 27 points with an interval 500 m, as is shown in Figure 14. This anomaly has been analyzed using the least-squares standard deviation method by Abdelrahman and Abo-Ezz [2008]. This anomaly was also investigated by several authors, such as Roy et al. [2000] which introduced a new concept in Euler deconvolution method to estimate the depth of the causative mass, Mehanee [2014] used the flair function minimization, Biswas [2015] proposed using very fast simulated annealing global optimization for interpreting the gravity anomaly and Singh and Biswas [2015] applied the global particle swarm optimization. The acquired solutions by the various method have been tabulated in Table 3.

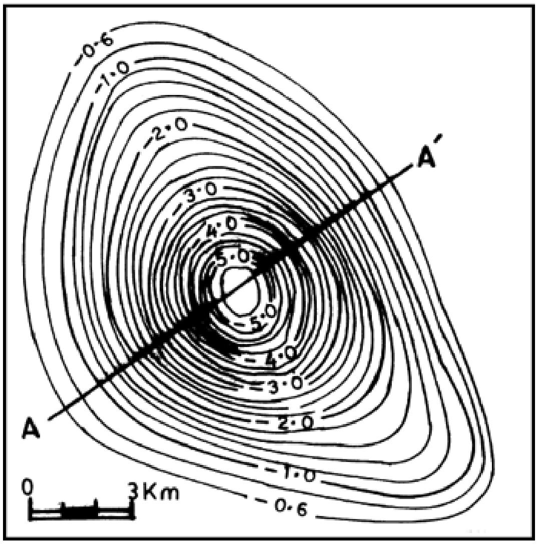


**Figure 12** The residual gravity anomaly map over offshore Louisiana salt dome, [Nettleton, 1976].

To compare, we apply the proposed method for this gravity anomaly, as the parameters values of the inferred structure using PSO are the radius (R)=578 m, depth to top (z)=1763 m, depth to bottom (h)=9185 m, location of mass ($x_0$) =427 m, gravity value in the origin ($g_{x0}$) =6.1 mGal and density contrast (ρ)=-1892 kg/m$^3$. Figure 13 shows the frequency distributions of the estimated parameters values in the several range of the solutions for the Louisiana salt dome.

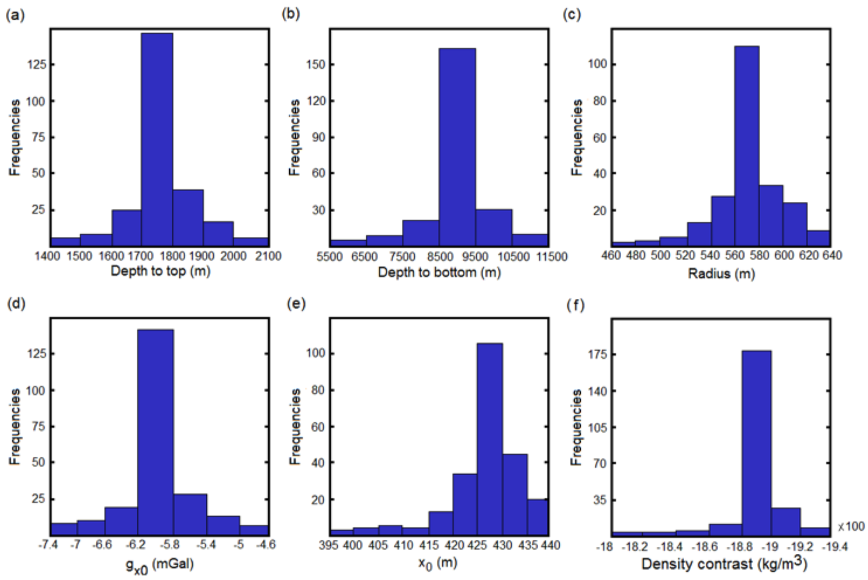


**Figure 13** Frequency distribution of the various parameters solutions a) depth to top (m) b) depth to bottom (m) c) radius (m) d) gravity value in the origin (mGal) e) location of mass (m) f) density contrast (kg/m$^3$) for real gravity data due to the Louisiana salt dome.

The obtained parameters from PSO inversion is given in Table 3. The gravity response caused by the inverted structure is displayed in Figure 14.

As several wells were drilled over this dome, detailed information is available [Nettleton, 1976]. The top of the dome was encountered in the shallowest well at 1.2 km up to a depth of around 1.8 km. Thus, the depth to top estimated by the least-squares standard deviation method [Abdelrahman and Abo-Ezz, 2008] and presented method based on PSO are closer to the reality.

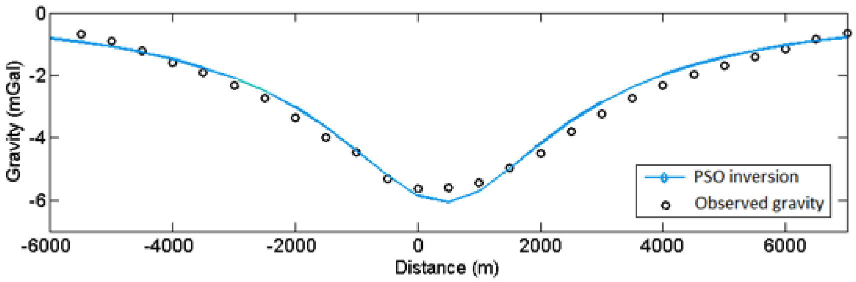


**Figure 14** The observed gravity anomaly due to Louisiana salt dome (black circles) and gravity responses from PSO inversion (blue curve).

| Parameter | | R (m) | h (m) | z (m) | $g_{x0}$ (mGal) | ρ (kg/m$^3$) | $x_0$ (m) |
|---|---|---|---|---|---|---|---|
| Estimated values | Roy et al. [2000] | - | 11300 | 2260 | - | - | - |
| | Abdelrahman and Abo-Ezz [2008] | - | 9287 | 1433 | - | - | - |
| | Mehanee [2014] | - | - | 2899 | - | - | - |
| | Biswas [2015] | - | - | 2702 | - | - | 506.5 |
| | Singh and Biswas [2016] | 436.43±129.91 | - | 2874.80±53.90 | - | -2510±121 | 451.02±24.63 |
| | Present method | 578 | 9185 | 1763 | 0.61 | -1892 | 427 |

**Table 3** The obtained parameters from the analysis of the Louisiana salt dome gravity data using various method.

# 6. Discussion and Conclusions

Presence of error in the geophysical inverse modeling and numerical computation is unavoidable, due to some factors such as the heterogeneity and discontinuity of the interior geological structures, the incoherence and incompatibility of the undersurface structures and masses configuration with various geometric shapes. Therefore, the proposed method is no exception as well. In this paper, we have proposed using Particle Swarm Optimization algorithm for the inverse modeling of the gravity data generated from a source with a geometric of the finite vertical cylinder. To resolve the weaknesses of PSO algorithm, that is, to fall into local minimum and inopportune convergence, a strategy based on the mean value of the maximum frequency distribution is applied. A prime advantage of the PSO is determination the maximum and minimum limits based on the geological and other geophysical information for the under surface structure variable parameters as the solutions do not exceed from the both of them and consequently the computational error and processing time extremely decrease and the optimal solution is achieved. Besides, PSO performance in the interpretation of gravity data is a non linear inversion process, thus can mostly eliminates the solution non uniqueness problem.
The proposed method was examined on synthetic gravity data related to a finite vertical cylinder model, with and without random noise. The obtained results from the PSO inversion are com-

pletely admissible as the inferred structure parameters are similar the assumed ones. Based on the objective function (equation 5) the evaluated errors between the computed theoretical gravity data, noise-free and noise corrupted synthetic data, and inverted one are 0.0036 and 0.061, respectively. The interpretation of the models verifies the PSO is an intelligent powerful tool for the inverse modeling of the gravity.
PSO was applied to analyze the real gravity data due to a chromite deposit mass from Iran. The inverted gravity from the computed parameters by the PSO shows an objective function error of 0.33 than the observed gravity. The estimated values for the depth to top, depth to bottom, radius and density contrast parameters of the subsurface gravity anomaly causative body using the PSO algorithm are 5.8 m, 80.4 m, 13.14 m and 1627 kg/$m^3$, respectively.
Furthermore, the PSO algorithm was employed to invert the 2-D residual gravity anomaly due to the offshore Louisiana salt dome from USA. The obtained values for the depth to top, depth to bottom, radius and density contrast parameters of the inferred structure using the PSO algorithm are 1763 m, 9185 m, 578 m and -1892 kg/$m^3$, respectively. The estimated depth to top has a good conformity with the drilling results. The objective function error between the measured gravity over the Louisiana salt dome and calculated gravity corresponding to the evaluated parameters by the PSO is about 0.03.

## References

Abdelrahman E.M. and Abo-Ezz E.R., (2008). *A Least-Squares Standard Deviation Method to Interpret Gravity Data due to Finite Vertical Cylinders and Sheets*. Pure Appl. Geophys., 165:947–965.

Alvarez J.P.F., Martinez F., Gonzalo E.G., Perez C.O.M., (2006). *Application of the particle swarm optimization algorithm to the solution and appraisal of the vertical electrical sounding inverse problem*. In Proceedings of the 11th Annual Conference of the International Association of Mathematical Geology (IAMG06), Liege, Belgium, CDROM.

Biswas A., (2015). *Interpretation of residual gravity anomaly caused by simple shaped bodies using very fast simulated annealing global optimization*. Geoscience Frontiers, 6, 875-893.

Singh A. and Biswas A., (2016). *Application of Global Particle Swarm Optimization for Inversion of Residual Gravity Anomalies Over Geological Bodies with Idealized Geometries*. Natural Resources Research, 4, 297-314.

Das S., Abraham A., Konar A., (2008). *Particle Swam Optimization and Differential Evolution Algorithms: Technical Analysis, Applications and Hybridization Perspectives*. Studies in Computational Intelligence (SCI), 116, 1–38.

Eshaghzadeh A., Dehghanpour A., Sahebari S.S., (2019). *Marquardt inverse modeling of the residual gravity anomalies due to simple geometric structures: A case study of chromite deposit*. Contributions to Geophysics and Geodesy, 49(2), 153–180.

Essa K.S. and Elhussein M., (2017). *2D dipping dike magnetic data interpretation using a robust particle swarm optimization*. Geosci. Instrum. Method. Data Syst. Discuss, 39.

Essa K.S. and Elhussein M., (2018). *Gravity Data Interpretation Using Different New Algorithms: A Comparative Study: Gravity-Geoscience Applications*. Industrial Technology and Quantum Aspect, Licensee InTech.

Essa K.S. and Elhussein M., (2018). *PSO (Particle Swarm Optimization) for Interpretation of Magnetic Anomalies Caused by Simple Geometrical Structures*. Pure Appl. Geophys., 175, 3539–3553.

Hammer S., (1974). *Graticule spacing versus depth discrimination in gravity interpretation*. Geophysics, 42, 60-65.

Heiland C.A., (1968). *Geophysical Exploration*. 2nd ed. Hafner Publishing Co., New York.

Kennedy J. and Eberhart R., (1995). *Particle swarm optimization*. IEEE International Conference

on Neural Networks 4, 1942–1948.
Mehanee S.A., (2014). *Accurate and efficient regularised inversion approach for the interpretation of isolated gravity anomalies*. Pure and Applied Geophysics, 171, 1897-1937.
Monteiro Santos F.A., (2010). *Inversion of self-potential of idealized bodies' anomalies using particle swarm optimization.* Computers & Geosciences, 36, 1185–1190.
Nettleton L.L., (1976). *Gravity and Magnetics in Oil Prospecting*. McGraw-Hill Book Co.
Pallero J.L.G., Fernández-Martínez J.L., Bonvalot S., and Fudym O., (2015). *Gravity inversion and uncertainty assessment of basement relief via Particle Swarm Optimization*. Journal of Applied Geophysics, 116, 180–191.
Parsopoulos K.E. and Vrahatis M.N., (2002). *Recent approaches to global optimization problems through particle swarm optimization*. Natural Computing, 1, 235–306.
Roshan R. and Singh U.K., (2017). *Inversion of residual gravity anomalies using tuned PSO*. Geosci. Instrum. Method. Data Syst., 6, 71–79.
Roy L., Agarwal B.N.P., Shaw R.K., (2000). *A new concept in Euler deconvolution of isolated gravity anomalies*. Geophysical Prospecting, 48, 559-575.
Shaw R. and Srivastava S., (2007). *Particle swarm optimization: a new tool to invert geophysical data*. Geophysics, 72, F75–F83.
Shi Y. and Eberhart R., (1998). *A modified particle swarm optimizer. In IEEE international conference on evolutionary computation.* IEEE Press, Piscataway, NJ, pp. 69–73.
Singh K.K. and Singh U.K., (2017). *Application of particle swarm optimization for gravity inversion of 2.5-D sedimentary basins using variable density contrast*. Geosci. Instrum. Method. Data Syst., 6, 193–198.
Sweilam N.H., El-Metwally K., Abdelazeem M., (2007). *Self potential signal inversion to simple polarized bodies using the particle swarm optimization method: A visibility study*. Journal of Applied Geophysics, 6, 195–208.
Toushmalani R., (2013a). *Comparison result of inversion of gravity data of a fault by particle swarm optimization and Levenberg–Marquardt methods*. SpringerPlus, 2, 462.
Toushmalani R., (2013b). *Gravity inversion of a fault by Particle Swarm Optimization (PSO).* SpringerPlus, 2, 315.
Yi L., (2016). *Study on an Improved PSO Algorithm and its Application for Solving Function Problem.* International Journal of Smart Home, 3, 51-62.

# QUADERNI di GEOFISICA

ISSN 1590-2595 http://istituto.ingv.it/it/le-collane-editoriali-ingv/quaderni-di-geofisica.html/

I QUADERNI DI GEOFISICA (QUAD. GEOFIS.) accolgono lavori, sia in italiano che in inglese, che diano particolare risalto alla pubblicazione di dati, misure, osservazioni e loro elaborazioni anche preliminari che necessitano di rapida diffusione nella comunità scientifica nazionale ed internazionale. Per questo scopo la pubblicazione on-line è particolarmente utile e fornisce accesso immediato a tutti i possibili utenti. Un Editorial Board multidisciplinare ed un accurato processo di peer-review garantiscono i requisiti di qualità per la pubblicazione dei contributi. I QUADERNI DI GEOFISICA sono presenti in "Emerging Sources Citation Index" di Clarivate Analytics, e in "Open Access Journals" di Scopus.

QUADERNI DI GEOFISICA (QUAD. GEOFIS.) welcome contributions, in Italian and/or in English, with special emphasis on preliminary elaborations of data, measures, and observations that need rapid and widespread diffusion in the scientific community. The on-line publication is particularly useful for this purpose, and a multidisciplinary Editorial Board with an accurate peer-review process provides the quality standard for the publication of the manuscripts. QUADERNI DI GEOFISICA are present in "Emerging Sources Citation Index" of Clarivate Analytics, and in "Open Access Journals" of Scopus.

# RAPPORTI TECNICI INGV

ISSN 2039-7941 http://istituto.ingv.it/it/le-collane-editoriali-ingv/rapporti-tecnici-ingv.html/

I RAPPORTI TECNICI INGV (RAPP. TEC. INGV) pubblicano contributi, sia in italiano che in inglese, di tipo tecnologico come manuali, software, applicazioni ed innovazioni di strumentazioni, tecniche di raccolta dati di rilevante interesse tecnico-scientifico. I RAPPORTI TECNICI INGV sono pubblicati esclusivamente on-line per garantire agli autori rapidità di diffusione e agli utenti accesso immediato ai dati pubblicati. Un Editorial Board multidisciplinare ed un accurato processo di peer-review garantiscono i requisiti di qualità per la pubblicazione dei contributi.

RAPPORTI TECNICI INGV (RAPP. TEC. INGV) publish technological contributions (in Italian and/or in English) such as manuals, software, applications and implementations of instruments, and techniques of data collection. RAPPORTI TECNICI INGV are published online to guarantee celerity of diffusion and a prompt access to published data. A multidisciplinary Editorial Board and an accurate peer-review process provide the quality standard for the publication of the contributions.

# MISCELLANEA INGV

ISSN 2039-6651 http://istituto.ingv.it/it/le-collane-editoriali-ingv/miscellanea-ingv.html

MISCELLANEA INGV (MISC. INGV) favorisce la pubblicazione di contributi scientifici riguardanti le attività svolte dall'INGV. In particolare, MISCELLANEA INGV raccoglie reports di progetti scientifici, proceedings di convegni, manuali, monografie di rilevante interesse, raccolte di articoli, ecc. La pubblicazione è esclusivamente on-line, completamente gratuita e garantisce tempi rapidi e grande diffusione sul web. L'Editorial Board INGV, grazie al suo carattere multidisciplinare, assicura i requisiti di qualità per la pubblicazione dei contributi sottomessi.

MISCELLANEA INGV (MISC. INGV) favours the publication of scientific contributions regarding the main activities carried out at INGV. In particular, MISCELLANEA INGV gathers reports of scientific projects, proceedings of meetings, manuals, relevant monographs, collections of articles etc. The journal is published online to guarantee celerity of diffusion on the internet. A multidisciplinary Editorial Board and an accurate peer-review process provide the quality standard for the publication of the contributions.

**Coordinamento editoriale e impaginazione**
Francesca DI STEFANO, Rossella CELI
Istituto Nazionale di Geofisica e Vulcanologia

**Progetto grafico e impaginazione**
Barbara ANGIONI
Istituto Nazionale di Geofisica e Vulcanologia

©2020
Istituto Nazionale di Geofisica e Vulcanologia
Via di Vigna Murata, 605
00143 Roma
tel. +39 06518601

**www.ingv.it**

Creative Commons Attribution 4.0 International (CC BY 4.0)

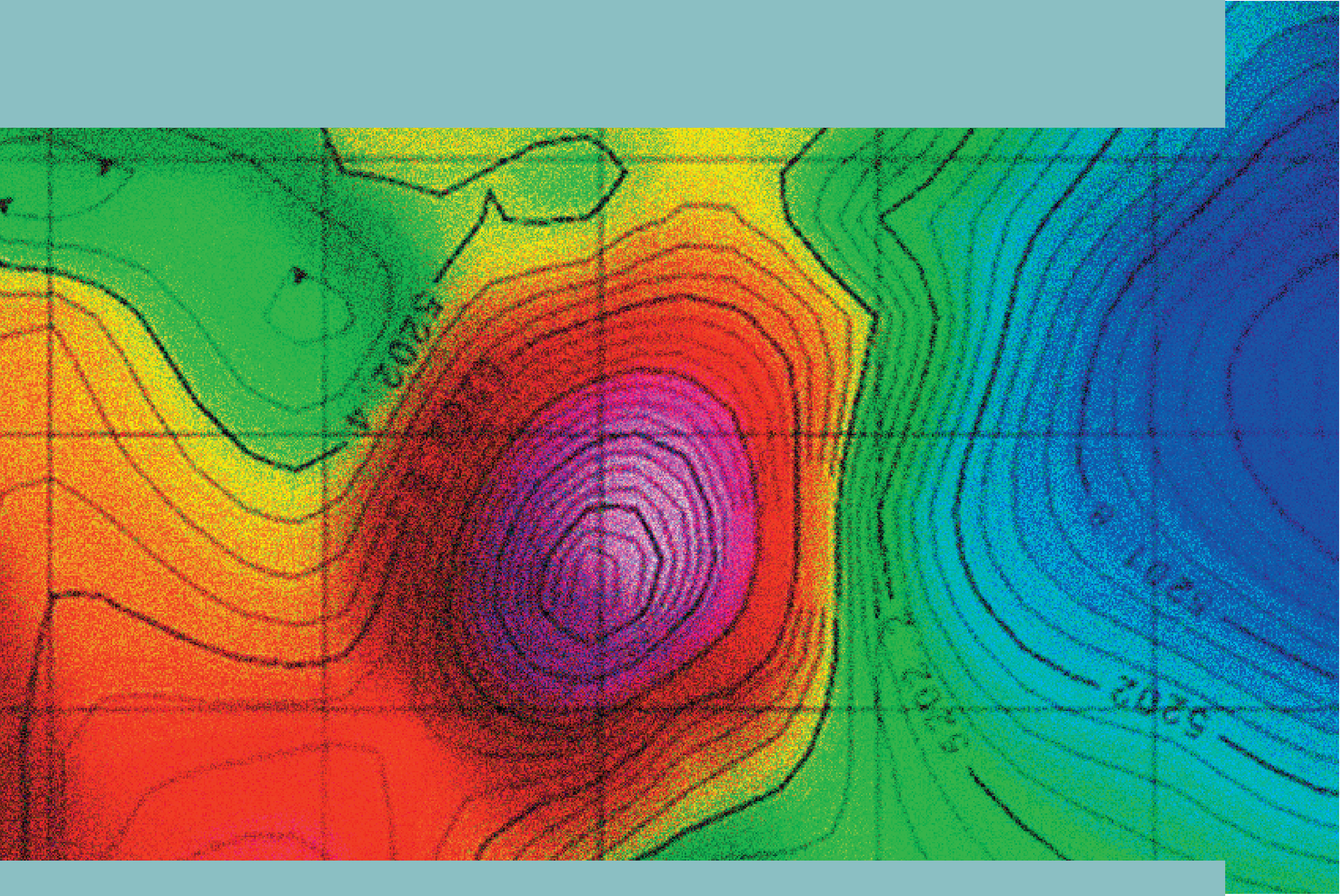

ISTITUTO NAZIONALE DI GEOFISICA E VULCANOLOGIA